Applied Catalysis A, General 544 (2017) 173–180

Contents lists available at ScienceDirect

Applied Catalysis A, General

journal homepage: www.elsevier.com/locate/apcata

Kinetic Modelling of the catalytic oxidation of 2-(methylmercapto)-benzothiazole under mild conditions

A. Córdoba*, C. Saux, L.B. Pierella

Centro de Investigación y Tecnología Química (CITeQ), UTN – CONICET, Maestro Marcelo Lopez y Cruz Roja Argentina, (5016) Córdoba, Argentina

ARTICLE INFO

Keywords:
Cu-Zeolites
2-(methylmercapto)-benzothiazole
H_2O_2 oxidation
Kinetic modelling

ABSTRACT

2-(Methylmercapto)-benzothiazole oxidation was performed over Copper modified zeolites. The microporous materials were synthesized by the hydrothermal crystallization method and later modified with metal incorporation by wet impregnation. The solid catalysts were characterized by means of X-ray diffraction, surface area determinations, inductively coupled plasma emission spectrophotometry, temperature programmed reduction and Fourier transformed infrared spectroscopy. Reaction parameters (Copper content, nature of the solvent, hydrogen peroxide concentration, reaction time, catalyst mass and reaction temperature) were evaluated to reach the optimum reaction conditions. Kinetic modelling and kinetic parameter estimation based on experimental kinetic data were included. Cu(II) species were confirmed as the active sites of the catalysts, being Y zeolite the optimal support. Thus, Fenton-like reaction mechanism with reactive oxygen species as hydroxyl and hydroperoxyl radicals ($HO\cdot$, $HO_2\cdot$) was confirmed. Reactions rates constants values and activation energy were determined by non-linear least-square parameter estimation. Also, homogeneous catalytic system was evaluated in order to discard diffusional limitations.

1. Introduction

It is well known that benzothiazole and its derivatives are normally found in the environment since they are used as fungicides, herbicides, corrosion inhibitors in cooling water for automobiles and as vulcanization accelerators in rubber production [1,2]. Considering their toxicity and extensive employment all around the world, their degradation study is of great environmental concern.

Among them, 2-mercaptobenzothiazole (2-MBT) is worldwide used as accelerator in vulcanization processes − since it catalyzes the formation of sulfide linkages between unsaturated elastomeric polymers in order to obtain a flexible and elastic crosslinked material [3] − and as a corrosion inhibitor in aqueous systems, as an ingredient in cutting oils and petroleum products and as an additive in extreme-pressure greases [4]. Its presence has been detected in wastewaters from rubber additive manufacturing, effluents from treatment plants and in rivers near to the rubber or tyre-manufacturing industries, but also in urban runoff, treated wastewater and even in urban air, probably because of tyre abrasion [5,6]. According to Reemtsma et al. [7], 2-MBT may undergo biologically-mediated methylation to form 2-(methylmercapto)-benzothiazole (2-MMBT), a typical breakdown product from benzothiazoles compounds. Actually, 2-MMBT is not effectively removed by current wastewater treatments and it has been found in groundwater and tap water, as a hint that it is not efficiently biodegraded, whereby additional treatments should be done [8]. In this sense, chemical treatments, in particular oxidation ones, seem to be the most appropriate in order to reduce contamination, considering that oxidation products (the corresponding sulfoxide and sulfone) are more biodegradable [9].

In "green" organic oxidations, modified zeolites have been employed as heterogeneous catalysts with positive results [10]. So, we propose the use of modified synthetic zeolites as active solid materials in order to mitigate this serious issue. It is well known the ordered organization of these aluminosilicate materials with a microporous structure consisting of a network of channels at a molecular scale. The presence of framework aluminum atoms makes these materials solid-acid catalysts. These properties make zeolites suitable for several catalytic applications [11].

Kinetic studies are always necessary in order to improve catalytic reactions, particularly for sulfides degradation, since they could help in the design of the reactive system. Several oxidation mechanisms have been proposed for zeolites as catalysts [12–15]. Reagents and products concentrations monitoring, allows inferring some issues about different reactions pathways. Kinetic modelling and parameter estimation by fitting experimental data (concentration vs. time) are useful tools in order to discern between different proposed mechanisms [16]. In

* Corresponding author.
E-mail address: acordoba@frc.utn.edu.ar (A. Córdoba).

http://dx.doi.org/10.1016/j.apcata.2017.07.001
Received 26 April 2017; Received in revised form 23 June 2017; Accepted 3 July 2017
Available online 08 July 2017
0926-860X/

addition, different approaches could be done to obtain the kinetics parameters-values, which could be further applied for reactors design purposes. Ramli and coworkers have recently reported a kinetic modelling of glucose decomposition catalyzed by Fe-Y zeolite [17]. The authors employed a pseudo first-order approach and linearization strategies in order to obtain rate constants values. Temperature effect was also determined by these approaches based on linear regressions procedures. Meanwhile, Hahn and co-workers have modelled the NH_3 oxidation on Fe-Beta zeolite employing stationary stage approach [18]. Arrhenius plots were used to evaluate temperature effects. Nevertheless, there are some assumptions which must be fulfill in order to obtain appropriate results [19]. One of these assumptions is the normal distribution of experimental errors. However, data transformations, as linearization strategies, do not guarantee the normal distribution of errors [19]. In order to avoid this limitation, non-linear least-square parameter estimation could be applied. Even though, some of that linearization approaches could be used to obtain initial values for non-linear least-square kinetics parameters estimation [20].

In this study, different Cu(II) modified zeolite matrices (ZSM-5, Y and Beta) are tested as heterogeneous catalysts for 2-MMBT/H_2O_2 oxidation. The synthesis procedure and post-synthesis modifications are described, as well as characterization results (XRD, TPR, BET, ICP and FTIR). Effects of zeolite matrix, Copper-charge, solvent and H_2O_2 concentrations are evaluated. A theoretical-experimental kinetic study for the optimal catalyst is also carried out. An oxidation mechanism is proposed and a dynamic modelling with parameter estimation by fitting experimental data is included. Furthermore, temperature effect by Arrhenius parameter estimation is evaluated. Finally, homogeneous vs heterogeneous catalytic oxidations are studied in order to evaluate mass transfer problems.

2. Experimental

2.1. Catalysts preparation

Zeolitic microporous materials were prepared following the hydrothermal crystallization procedure for ZSM-5 and Beta. The ammonium form of Y zeolite was purchased from Sigma-Aldrich.

In the case of Na-ZSM-5, it was obtained in the Na_2O-Al_2O_3-SiO_2 system, using TPAOH (Tetrapropylammonium Hydroxide, Fluka) as a structure directing agent by known methods [21] with some modifications made by our group.

The Na-Beta was synthesized by means of the hydrothermal crystallization method using Tetraethylammonium Hydroxide (Merck) as directing agent following the method reported by Valencia et al. [22].

In both cases, the structure directing agent was desorbed in N_2 atmosphere (20 ml/min) at programmed temperature (10 °C/min) from room temperature to 500 °C for 8 h and then were calcined in air at 500 °C for 12 h. The ammonium forms of the catalysts were obtained by ion-exchange of the Na-zeolites with NH_4Cl (Fluka, 1 M) for 40 h at 80 °C in a batch reactor with continuous mechanical agitation.

The ammonium matrices (NH_4-zeolites) were suspended in a solution of $Cu(C_2H_3O_2)_2{\cdot}H_2O$ (Mallinckrodt) in the least amount of distilled water in order to obtain the desired Copper content. Water was further evaporated using a rotator–evaporator at 80 °C under vacuum until complete dryness. After that, the samples were dried at 110 °C and desorbed in N_2 flow (10 ml/min) at programmed temperature (10 °C/min) from room temperature to 500 °C for 12 h followed by calcination in air at 500 °C for 12 h.

2.2. Catalysts characterization

Chemical composition was determined by using an inductively coupled plasma emission spectrophotometer Varian 715ES. BET surface area determinations were carried out with an ASAP 2000 equipment. Phase purity of the catalysts was determined by X-ray diffraction (XRD) in a Philips X'Pert MPD diffractometer equipped with a PW3050 goniometer (CuKα radiation, graphite monochromator), provided with a variable divergence slit and working in the fixed irradiated area mode. Diffraction data were recorded between $2\theta = 4°$ and 40° at an interval of 0.05°. A scanning speed of 2°/min was used.

Infrared measurements in the lattice vibration region (400–1800 cm^{-1}) were performed on a JASCO 5300 FTIR spectrometer using KBr 0.05% wafer technique. In order to determine the acid sites of the samples self-supporting wafers were done and a spectral scanning from 4600 to 400 cm^{-1} in 16 consecutive registers of 4 cm^{-1} resolution were performed. The wafers were heated at 400 °C in vacuum (10^{-4} Torr) for 6 h and then pyridine (3 Torr) was adsorbed at room temperature for 12 h and desorbed for an hour at 350 °C at 10^{-4} Torr. The experiments were carried out using a thermostatized cell with CaF_2 windows connected to a vacuum line.

Temperature programmed reduction (TPR) studies were done over calcined Cu-containing zeolites in an Autochem 2910 Micromeritics equipment. Typically, 100–160 mg of pelletized samples (0.2–0.4 mesh) were used in order to have a constant weight of Copper in all the samples. Samples were firstly pre-treated under Argon flow (50 ml/min) at room temperature during 15 min. Then, gas flow was changed to 10% H_2/Ar (50 ml/min) and temperature was raised from 25 to 800 °C at 10 °C/min using a computer-controlled program. The hydrogen uptake was monitored by means of a TCD detector connected on-line, and data will present the evolution of TCD signal in function of the increasing in temperature. Calibration of the equipment was made under same experimental conditions using CuO as reference sample.

2.3. Catalytic activity

2-(Methylmercapto)-benzothiazole (2-MMBT) (97%, Aldrich) oxidation reactions were performed employing H_2O_2 (aqueous solution 30 wt%, Cicarelli) as oxidant agent in a glass flask reactor (25 cm^3) with magnetic stirring immersed in a thermostatized bath, equipped with a reflux condenser. The standard catalytic tests were done at 40 °C during 5 h, in a 2-MMBT/hydrogen peroxide molar ratio of 0.1, employing acetonitrile (99.5%, Cicarelli) as solvent and 100 mg of the selected catalyst. Nevertheless, temperature was varied from 25 to 60 °C, solvents of different characteristics (polarity and proticity) were tested and different types of catalysts and concentrations were also evaluated.

The reaction evolution was followed by taking aliquots of the solution at different reaction times. Products were identified by mass spectrometry GC- Mass (Shimadzu QP 5050 GC–17 A) and quantified by gas chromatography (Perkin Elmer Clarus 500). The solid catalysts were filtrated before the analysis of the products. The substrate conversions are reported as mol%.

In order to determine diffusional problems of substrates into zeolites cavities, an homogenous catalytic reaction was done employing Cu $(CH_3COO)_2$ as catalyst, maintaining constant the same 2-MMBT/Cu ratio and the standard reaction conditions.

2.4. Kinetic modelling and parametrization

Based on catalytic activity results presented in Section 3.2, Cu(3)Y was selected for the Kinetic modelling and parametrization study. Initial rates analysis of 2-MMBT oxidation catalyzed by Cu-Y were carried on. Experimental data (concentration vs. time) has been fitted to double-exponential curves and the initial rates were determined by $(dC/dt)_{t=0}$.

The incorporation of different transition metals on zeolites matrices enables their use in many kinds of reactions. Among them, heterogeneous Fenton and Fenton-like catalysts could be obtained from transition metal-zeolites [23,24]. Fenton reaction systems are based on HO· production from H_2O_2 in presences of Fe(II)/Fe(III) species. However, Cu(I)/Cu(II) can catalyse hydroxyl radical formation

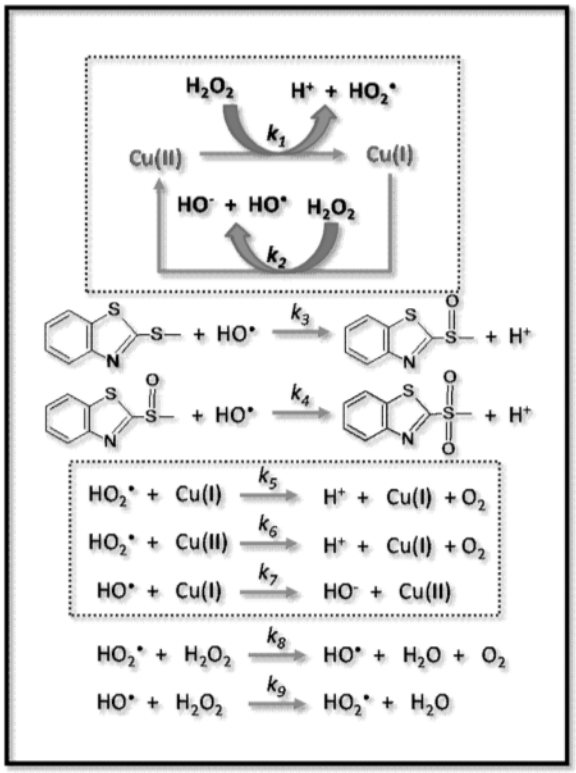

Scheme 1. Proposed reaction mechanism for Cu/2-MMBT/H_2O_2 catalytic system.

−among other oxygen reactive species (ROS)- in presence of H_2O_2 [24–26]. Organic compounds can be oxidized by highly reactive hydroxyl radical ($E^{\circ}_{(HO\cdot/H2O)} = +2{,}8\ V_{NHE}$) [27–29]. Wang et al. have reported evidence of hydroxyl radical formation catalyzed by Cu-Y zeolites in phenol hydroxylation with H_2O_2 [29]. Based on Cu(I)/Cu(II) Fenton-like system, an oxidation pathway for 2-MMBT/H_2O_2/Cu-modified zeolites is proposed (Scheme 1). The model considers Cu as the active specie of the catalyst and formation of the hydroxyl and hydroperoxyl radical (HO·, HO_2·) over it.

Mathematical model (Eqs. (1)–(10)) was obtained by mass balance of all the involved species (2-MMBT and its oxidized products −P1: sulfoxide, P2: sulfone-, catalytic intermediaries and reaction intermediaries). Arrhenius model (Eq. (11)) was employed to evaluate the temperature effect, considering 40 °C as reference temperature.

$$\frac{d[Cu(II)]}{dt} = -k_1[H_2O_2][Cu(II)] - k_6[HO_2^{\bullet}][Cu(II)] + k_2[H_2O_2][Cu(I)] + k_5[HO_2^{\bullet}][Cu(I)] + k_7[HO^{\bullet}][Cu(I)] \quad (1)$$

$$\frac{d[Cu(I)]}{dt} = k_1[H_2O_2][Cu(II)] + k_6[HO_2^{\bullet}][Cu(II)] - (k_7[HO^{\bullet}] + k_5[HO_2^{\bullet}] + k_2[H_2O_2])[Cu(I)] \quad (2)$$

$$\frac{d[MMBT]}{dt} = -k_3[HO^{\bullet}][MMBT] \quad (3)$$

$$\frac{d[H_2O_2]}{dt} = -k_1[H_2O_2][Cu(II)] - k_2[H_2O_2][Cu(I)] - k_8[H_2O_2][HO_2^{\bullet}] - k_9[H_2O_2][HO^{\bullet}] \quad (4)$$

$$\frac{d[P1]}{dt} = k_3[HO^{\bullet}][MMBT] - k_4[HO^{\bullet}][P1] \quad (5)$$

$$\frac{d[P2]}{dt} = k_4[HO^{\bullet}][P1] \quad (6)$$

$$\frac{d[O_2]}{dt} = k_6[HO_2^{\bullet}][Cu(II)] \quad (7)$$

$$\frac{d[HO^{\bullet}]}{dt} = k_2[H_2O_2][Cu(I)] + k_8[H_2O_2][HO_2^{\bullet}] - k_9[H_2O_2][HO^{\bullet}] - k_3[MMBT][HO^{\bullet}] - k_4[P1][HO^{\bullet}] - k_7[Cu(I)][HO^{\bullet}] \quad (8)$$

$$\frac{d[HO_2^{\bullet}]}{dt} = k_1[H_2O_2][Cu(II)] + k_9[H_2O_2][HO^{\bullet}] - k_8[H_2O_2][HO_2^{\bullet}] - k_5[Cu(I)][HO_2^{\bullet}] - k_6[Cu(II)][HO_2^{\bullet}] \quad (9)$$

$$\frac{d[HO^-]}{dt} = k_7[Cu(I)][HO^{\bullet}] + k_2[H_2O_2]Cu(I) \quad (10)$$

$$k_T = k_{T_r}\exp\left[-\frac{E_a}{R}\left(\frac{1}{T}-\frac{1}{T_r}\right)\right] \quad (11)$$

Multiresponse modelling of the proposed mechanism was carried on employing commercial software g-PROMS 3.2 (General PROcess Modelling System, Process System Enterprise Ltd., London, United Kingdom). g-PROMS parameter estimation tool, which assume independent and normally distributed experimental errors, were used. Kinetic and variance models were simultaneously optimized. A constant variance model was selected ($\sigma^2 = \omega^2$). Initial guesses of rate constants were obtained from literature. Also, intermediaries and reaction products initial concentrations were set at zero. The accuracy of the model was evaluated by X^2 (95%) test.

In order to evaluate mass transfer limitations the parametrization of heterogeneous and homogeneous experimental data were done in two steps and the resulting kinetic constants optimized values were evaluated.

Finally, the parametrization, including temperature effect, was carried on to obtain Arrhenius constants values.

3. Results and discussion

3.1. Cu-zeolites characterization

Copper modified zeolites (Cu-ZSM-5, Cu-Beta and Cu-Y) were characterized by different techniques. Table 1 summarizes physicochemical characterization results. It is well known that when a metal is incorporated on a porous material, the surface area could be diminished due to some pores blockage and metal sintering during the calcination step [30]. Nevertheless, just a slight reduction in surface area values calculated by the BET method were obtained.

In order to compare the zeolitic matrix effect on the catalytic activity, the same Copper content was impregnated over the different porous solids. As it could be seen from ICP results, about a 3 wt% was effectively loaded in each sample.

H_2-TPR results presented in Table 1 shown that Copper species in the matrices could be divided into two groups based on the reducibility of Cu ions. In the literature [31,32], it was suggested that Cu^{2+} is

Table 1
Physicochemical analysis of Cu-zeolites.

Sample	Si/Al[a]	Cu wt%[a]	Cu/Al[a]	S_{BET} (m^2/g)[b]	H_2 consumption[c]	
					$T_{a\,maximum}$ (°C)	(ml/g)
Cu-ZSM-5	19.93	2.99	0.68	337	202 (326)	10.01
Cu-Beta	10.51	3.14	0.39	525	220 (300)	13.34
Cu-Y	2.41	3.38	0.15	655	300 (201)	12.76

[a] Measured by inductively coupled plasma emission spectrophotometer (ICP).
[b] Determined by BET.
[c] Obtained from TPR measurements. (T): Temperature at maximum of the minor signal.

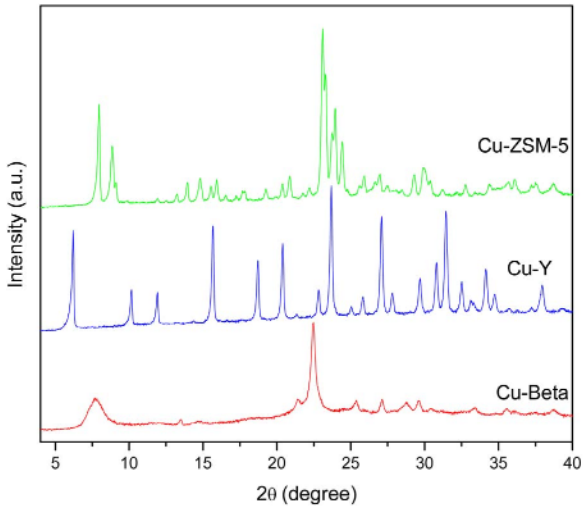

Fig. 1. X-ray diffraction patterns of fresh Cu-zeolites.

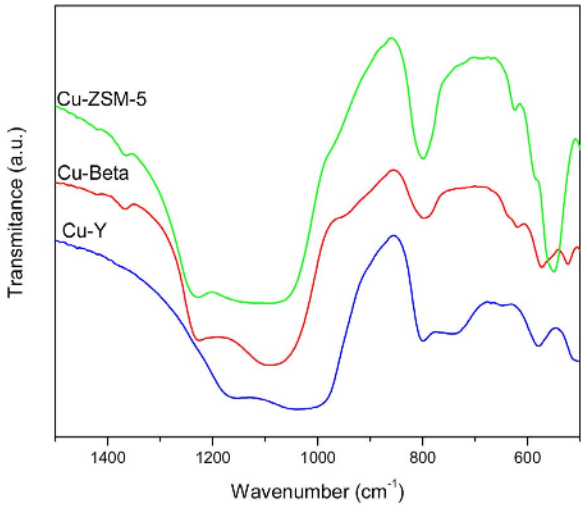

Fig. 2. FTIR spectra of Cu-modified zeolites (fresh samples) in the fingerprint region.

reduced to Cu^{+} at 200 °C, while Cu^{+} is reduced to Cu^{0} at 315 °C for ZSM-5 and Beta matrices. In the case of Cu-Y zeolite, the two reduction peaks observed at 201 °C and 300 °C are only attributed to the reduction of Cu^{2+} to Cu^{+} ions inside faujasite supercages (201 °C) and inside sodalite cages (300 °C), as found in literature [32,33]. It should be mentioned that Cu-Y sample presented the highest Cu^{2+} concentration of the evaluated matrices, according to TPR results. This is consistent with ICP results presented in Table 1, considering the fact that each isolated Cu^{2+} must be charge-compensated by two framework Al tetrahedral sites [34]. So, the density of these species is inversely proportional to Cu/Al molar ratio, that is the lowest for Cu-Y sample. This hypothesis was confirmed by the studies of Paolucci et al. for Cu exchange zeolite SSZ-13 where authors reported single metal ions, or $[Cu\text{-}OH]^{+}$ species over zeolite surface [35,36]. Even more, Göltl and coworkers have recently published studies focus in the active sites nature in Cu- zeolite SSZ-13. They showed that Copper can be as monovalent or bivalent cation. However, at low Si/Al ratios, the principal metal active site is Cu^{2+} because of the abundant presence of tetrahedral Al [37,38].

According to XRD patterns (Fig. 1), zeolites structures were preserved after Copper incorporation and all the thermal treatments applied to the materials, as evidenced by the characteristic reflexes presence in each sample. The absence of signals corresponding to crystalline Copper oxide phases could be due to small particle sizes (< 4 nm) or that the ions are at exchanged positions in the zeolites.

FTIR spectra of the samples in the fingerprint zone (1500–500 cm^{-1}) are shown in Fig. 2. As could be seen, Copper incorporation did not alter the structures of the zeolites, confirming XRD results. The well-defined bands at 800 and 1000–1300 cm^{-1} are assigned to the υ_s(T−O) and υ_{as}(T−O) stretching of Si−O(Al) vibration in tetrahedra, respectively [24,39,40], characteristics of these kind of structures.

It is well known the identification and quantification of acid sites by the adsorption of a probe molecule, as pyridine, followed by FTIR spectroscopy. Fig. 3 shows the IR spectra of the Cu-zeolites after pyridine adsorption and further desorption at 350 °C for an hour at 10^{-4} Torr of vacuum. It is possible to observe the bands corresponding to υ 19 B mode (1456 cm^{-1}) and υ 8A mode (1612 cm^{-1}), corresponding to pyridine interaction with Lewis acid sites, and the bands indicative of the interaction with Brönsted acid sites in the υ 19 B mode (1547 cm^{-1}) and υ8A mode (1635 cm^{-1}) [41]. According to the spectra, Cu-Y presents a higher concentration of Brönsted acid sites than the other matrices, while Lewis acid sites are similar to that obtained for Cu-Beta.

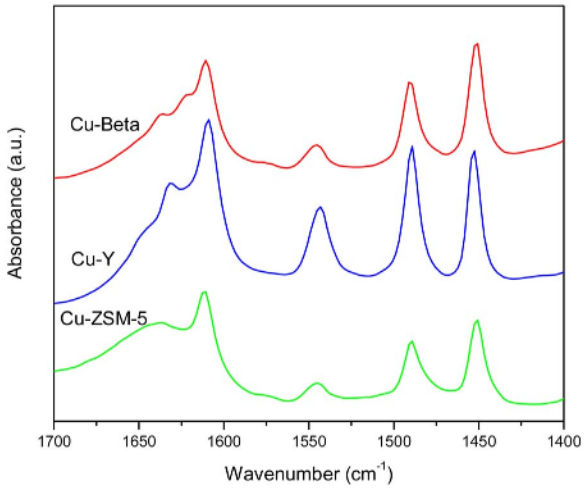

Fig. 3. FTIR spectra of pyridine adsorbed at room temperature and desorbed at 350 °C and 10^{-4} Torr over Cu-zeolites (fresh samples).

3.2. Catalytic activity

The oxidation of 2-MMBT employing hydrogen peroxide as oxidant was selected as model reaction in order to evaluate this kind of contaminant degradation. The selection was the result of studying Cu-zeolites catalytic behavior and reaching the optimal reaction conditions for this class of oxidation. Thus why, all the Copper modified matrices were tested at 40 °C, employing 0.1 g of catalyst, acetonitrile as solvent and a substrate/oxidant molar ratio of 0.1, as standard conditions. It should be noted that when the reaction was done without catalyst, the final sulfide conversion after 5 h of reaction was just 9 mol%. Fig. 4 shows the sulfide conversion results obtained for the different zeolite matrices evaluated and the non-catalytic reaction. Cu-Y is the most active material in order to convert 2-MMBT in its corresponding sulfoxide and sulfone, the major obtained products, reaching a 98 mol% of conversion at the end of the reaction.

From the above results, Y matrix was selected as the optimal support for Copper. Considering that Cu-Y showed the highest total acidity, a stabilizing effect of acid sites for Copper species could be proposed, as previously reported by Wang and coworkers [42], that favors the Fenton-like oxidation mechanism (Scheme 1). In this sense, under the conditions specified in Fig. 4, the evolution of the oxidation as function of reaction time was evaluated and the results are presented on Fig. 5.

As could be seen in the figure, as 2-MMBT reacts and its conversion increases with reaction time, the sulfoxide is obtained as primary

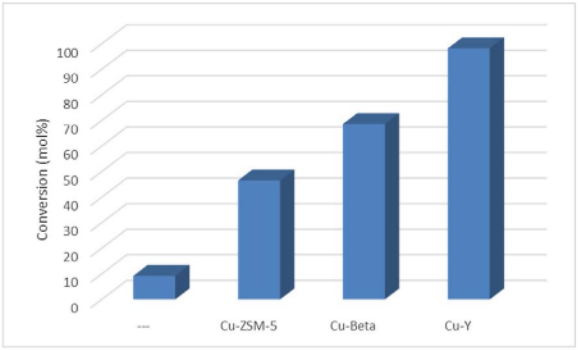

Fig. 4. Zeolite matrices evaluation for 2-MMBT conversion. Reaction conditions: catalyst mass (0.1 g), acetonitrile as solvent, sulfide/H_2O_2 molar ratio: 0.1, after 5 h at 40 °C.

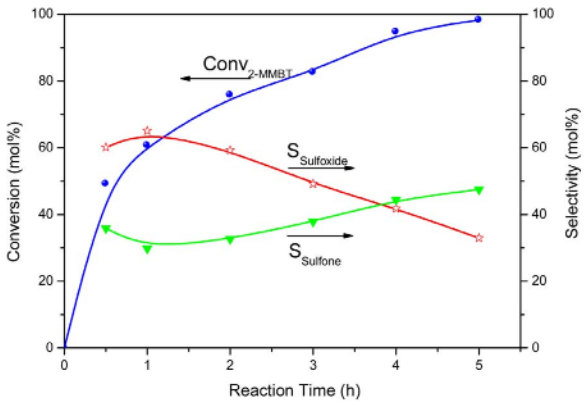

Fig. 5. Reaction evolution when Cu-Y was employed as catalyst. Reaction conditions: acetonitrile as solvent; catalyst mass: 0.1 g; sulfide/H_2O_2 molar ratio: 0.1; 40 °C.

oxidation product (P1), which is further re-oxidized to form the sulfone (P2), as proposed in the reaction Scheme 1. Finally, a 98 mol% of 2-MMBT conversion is reached with selectivities of 33 and 48 mol% to P1 and P2, respectively, after 5 h of reaction. Looking forward to confirm this proposed mechanism, where Copper species seem to be the active sites, the reaction was catalyzed by the protonic form of the zeolite matrix (H-Y) and just a 14 mol% of 2-MMBT conversion was obtained after 5 h of reaction, confirming that dispersed Copper species are the active sites of the catalyst. Nevertheless, this high surface area material is an optimal support that cooperates in the catalytic activity, since the final conversion obtained employing H-Y was a 5 mol% higher than the non catalytic reaction.

Many authors have studied solvent effect on heterogeneous catalysis [14,43,44], since its characteristics would affect in a significant way the reaction development. In this sense, a group of common organic molecules of different polarity and proticity properties (Acetonitrile, Ethanol, n-Hexane, 2-Butanol) were tested as solvents, maintaining the other reaction variables in the standard conditions, and the results after 5 h of reaction are presented in Fig. 6 as function of the Dielectric Constant of each solvent.

A linear enhancement on 2-MMBT conversion values was obtained as the polarity of the solvent increases. In fact, the highest conversion values were achieved employing Acetonitrile as solvent (highest Dielectric Constant). This aprotic solvent favors reactant interaction with the hydrophilic surface of the catalyst, facilitating its access to the Copper active sites.

When reaction temperature effect on sulfide conversion and products selectivities was studied (Fig. 7), a considerable increase on 2-MMBT conversion (27 mol%) was observed in the variation from room temperature to 40 °C. A similar behavior was obtained for sulfone selectivity at the cost of sulfoxide. Liu and coworkers attributed this behavior to the increase in H_2O_2 decomposition into highly reactive OH

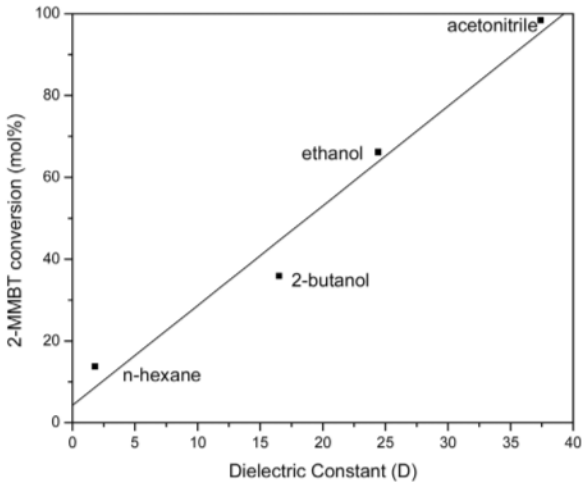

Fig. 6. Solvent effect on 2-MMBT conversion. Reaction conditions: sulfide/H_2O_2 molar ratio: 0.1, Cu-Y (0.1 g), after 5 h at 40 °C.

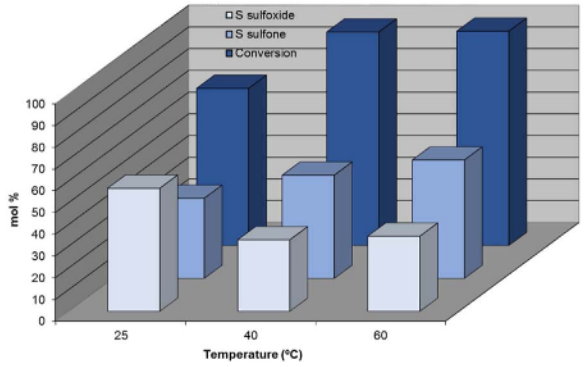

Fig. 7. Reaction Temperature Effect. Reaction conditions: 2-MMBT/H_2O_2 molar ratio: 0.1, Cu-Y: 0.1 g, acetonitrile as solvent, reaction time: 5 h.

· radicals with increase in temperature [45]. However, when a further increment on temperature was done to 60 °C, just a slight variation on sulfone selectivity was reached.

3.3. Kinetic modelling and parametrization

Effects of Copper loading (1–10 wt%), hydrogen peroxide concentration (2–5 M) and catalyst mass (0.02–0.2 mg) are summarized in Fig. 8 for Cu-Y. Fig. 8.a shows the non-linear dependency of $-r_{2\text{-MMBT}}$ with metal loading. The initial reaction rate shows a lineal dependency with Copper content at loadings lower than 3 wt%. At higher metal loading, reaction rate remains almost constant. These results could be assigned to the nature of Copper species over zeolite matrix. Paolucci and co-workers have studied Copper active sites and concluded that in catalysts with Cu/Al < 0,2 all Copper sites are equivalents. Beyond, at high Cu content the authors assigned the catalytic activity decrease of Cu-zeolite to the presence of Cu-OH species at Copper content > 3% [35]. Nevertheless, higher size Copper clusters on the zeolite surface, when higher metal content is incorporated, may produce mass transfer problems by the blockage of some pores mouths [24,30]. Thus, 3 wt% is the optimal metal incorporation in order to improve catalytic activity and it was selected for further analysis.

Catalytic nature of the oxidation was confirmed by the linear dependency of $-r_{2\text{-MMBT}}$ with Cu-Y mass, as expected (Fig. 8b). Nevertheless, a low non-catalytic oxidation rate was measured, corresponding to 0 mg of Cu-Y.

The linear dependency of $-r_{2\text{-MMBT}}$ with $[H_2O_2]$ indicates a first order reaction (Fig. 8.c). This result is in agreement with the proposed oxidative mechanism (Scheme 1). In order to confirm the radical

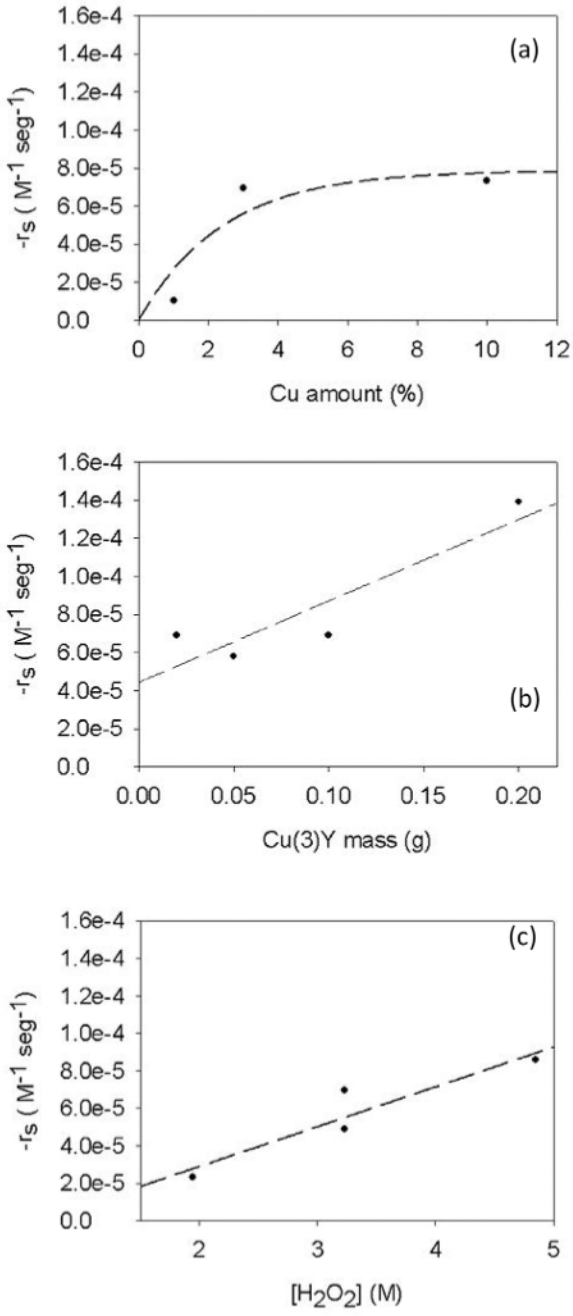

Fig. 8. Initial rates plots. (a) 2-MMBT oxidation rate vs Cu amount (wt%), (b) 2-MMBT oxidation rate vs catalyst mass, (c) 2-MMBT oxidation rate vs $[H_2O_2]$.

oxidation pathway proposed, a radical scavenger (isopropyl alcohol) was added to the reaction mixture after 30 min of reaction and 2-MMBT conversion was followed as function of time. It was noticeable that when the radical scavenger was incorporated, 2-MMBT conversion practically did not vary, showing just a 10 mol% of increment in the next 270 min of reaction.

Table 2 presents the obtained results for the parametrization procedure of the proposed mechanism (Scheme 1). The model accuracy to fit experimental data was demonstrated by $\chi^2(95\%) >$ weighed residuals. Furthermore, the parameter estimation gave meaningful values for k_1, k_3 and k_4. The obtained value of k_1 indicates that global reaction rate is controlled by the Cu(II) activation step. In addition, constants of 2-MMBT and sulfoxide oxidation steps (k_3 and k_4) are in accordance to the high reactivity of the OH· radicals [27–29].

Fig. 9 shows modelled and experimental concentrations profiles of

Table 2
Initial guesses and optimized rate constants values.

($M^{-1}\,s^{-1}$)	Initial guess ($M^{-1}\,s^{-1}$)	Optimized ($M^{-1}\,s^{-1}$)
k_1	0.002[a]	0.0016 ± 0.0003
k_2	7.6×10^{6} [a]	7.6×10^{6}
k_3	4.0×10^{9} [b]	$4.0 \times 10^{9} \pm 6.5 \times 10^{3}$
k_4	4.0×10^{9} [b]	$4.0 \times 10^{9} \pm 6.0 \times 10^{3}$
k_5	1.2×10^{8}[a*]	–
k_6	3.2×10^{5}[a*]	–
k_7	5.0×10^{8}[a*]	–
k_8	3.1 [a*]	–
k_9	2.1×10^{9}[a*]	–
E_a	15000	$465.49 \pm 136\,J\,mol^{-1}$
Initial guess of σ^2		0.01
Optimized σ^2		0.04 ± 0.003
Residuals		158.5
X^2 (95%)		183.96

*Fixed values during parametrization.
[a] From [46].
[b] From [47].

2-MMBT and its oxidized products. Model ability to fit experimental data could be observed in Fig. 9c and d. Moreover, experimental profiles corresponding to higher Copper concentrations had been successfully fitted (Fig. 9e). However, reaction rate is over-estimated at low catalyst concentration (Fig. 9a). Probably, non-catalytic oxidation pathways, not included in the proposed model, can become more important at these conditions. Some authors have modelled the effect of acid catalysts in oxygen atom transfer from H_2O_2 to a nucleophile as H_2S or $(CH3)_2S$. They conclude that weak acid catalysts can acts on the activation of O—O bond cleavage and favors the sulfides oxidation [48]. It is possible that at low metal content, the acid sites of the zeolitic matrix, catalyse H_2O_2 activation.

In order to evaluate the temperature effect over k_1, Arrhenius equation has been included into the model parametrization. Activation energy value (E_a) was determined (see Table 2). The obtained value is lower than those reported for homogeneous Fenton reactions witch vary from 8000 to 70000 J mol^{-1} as function of the reaction medium and the organic substrate that was oxidized [49–51]. However, this result is consistent with the proposed radical oxidation mechanism [52,53], improved by Copper stabilization through the acid matrix.

3.4. Homogeneous catalytic system

In order to evaluate the effect of Copper on catalysts activity, and the potential diffusion problems, activities measurements and rate constants estimations were carried on for systems catalyzed by soluble Cu(II) ($Cu(CH_3COO)_2$). Rate constant k_{1hom} was estimated by the parametrization procedure for homogenous experiments. Fig. 9.f and g show the agreement between experimental vs modelled 2-MMBT and its oxidized products evolution. The obtained k_{1hom} rate constant (k_{1hom}: 0.0008 ± 0.0001) is lower than the optimized k_1 value for the heterogeneous system. This result allows us to discard any diffusion limitations. Also, confirming the proposed oxidation model in which the small size H_2O_2 molecules are the species that diffuse into the zeolite channels. Moreover, the lower value obtained for the homogeneous rate constant, suggests that there is a synergic effect of the zeolite matrix over Copper catalytic activity, as probed when H-Y was evaluated as catalyst. Similar results were obtained in partial methane oxidation catalyzed by Cu-SSZ-13 zeolites. In fact, authors assigned this behavior to the environment generated by Copper confinement effect into the zeolite channels [37,38].

4. Conclusion

Different Copper-zeolites (ZSM5, BETA and Y) were evaluated as

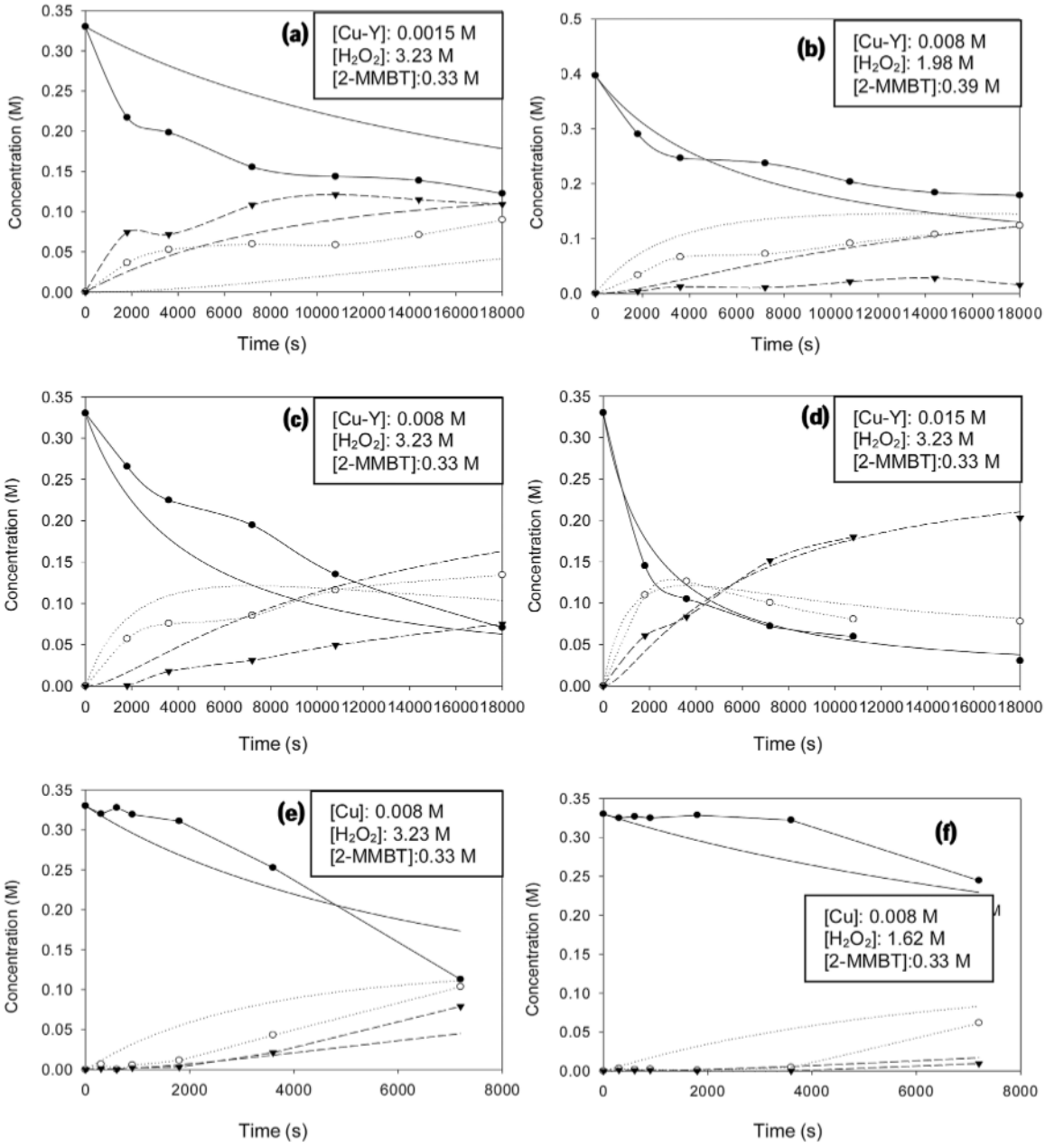

Fig. 9. Experimental (points) and modelled (lines) concentration profiles of 2-MMBT (continues lines) and its oxidized products (sulfoxide: dotted lines, sulfone: dashed line).

heterogeneous catalysts on the 2-MMBT/H_2O_2 oxidation reaction. According to ICP and H_2-TPR characterization results, Cu-Y sample presented the highest Cu^{2+} concentration. When the materials were tested in the reaction, Cu-Y showed the highest catalytic activity, which is consistent with the proposed reaction mechanism, where Cu^{2+} are the active sites in the catalyst. It was also confirmed employing H-Y as catalyst and obtaining low sulfide conversion. Even more, FTIR spectra showed that Copper incorporation preserved the zeolites structures and when pyridine was adsorbed and acid sites were analysed, Cu-Y presented the highest Brönsted acid sites concentration. This result allows us to propose a stabilizing effect of these acid sites over Copper species.

In order to select the optimal 2-MMBT/H_2O_2 catalytic oxidation system, different factors effects, as zeolite matrix, solvent-medium, reaction time and temperature, had been considered. Cu-Y was selected as the best catalyst since it showed a 98 mol% of 2-MMBT conversion after 5 h of reaction. On the other hand, a linear dependency of 2-MMBT conversion vs dielectric constant was obtained. Being Acetonitrile the solvent that showed better oxidation results, probably due to a positive effect of this aprotic and polar solvent on hydrophilic catalyst surface − reactants interaction.

Kinetic modelling and parametrization results also confirmed the proposed oxidation mechanism, with ROS formation, in concordance with experimental data. Thus, the obtained value of k_1 indicates that Cu (II)/H_2O_2 activation is the rate controlling step. Further, a low effect of temperature over this rate constant was obtained by the parameterization of Arrhenius equation.

Finally, parametrization of homogeneous data allow us to discard diffusional problems. Otherwise, a synergic effect of zeolite matrix on 2-MMBT conversion was confirmed according to the stabilizing effect proposal.

Acknowledgements

The authors thank Dr. Marcelo Domine from ITQ for XRD and TPR measurements of the samples. Additionally, the authors thank Dr. Mariano Asteasuain and Dra. Adriana Brandolín for their collaboration

in the activities related to gPROMS calculations.

This project was partially supported by: FONCYT PICT 2014- 1631, CONICET PIP11220130100146CO and UTN PIDUTI3864TC. We would also wish to thank CONICET.

References

[1] H. De Wever, H. Verachtert, Water Res. 31 (1997) 2673–2684.
[2] J.E. Grebel, J.A. Charbonnet, D.L. Sedlak, Water Res. 88 (2016) 481–491.
[3] Encyclopedia of Polymer Science and Technology/14. Thermogravimetric Analysis to Wire and Cable Coverings, Interscience Publ, 1971.
[4] M.H. Whittaker, A.M. Gebhart, T. Clipson Miller, F. Hammer, Toxicol. Ind. Health 20 (2004) 149–163.
[5] International Agency for Research on Cancer, World Health Organization, Q & A on 2 – Mercaptobenzothiazole (MBT), (2016).
[6] Y. Wan, J. Xue, K. Kannan, J. Hazard. Mater. 311 (2016) 37–42.
[7] T. Reemtsma, O. Fiehn, G. Kalnowski, M. Jekel, Environ. Sci. Technol. 28 (1995) 478–485.
[8] Y. Wang, J.K. Schaefer, B. Mishra, N. Yee, Environ. Sci. Technol. 50 (2016) 11049–11056.
[9] C.O. Kinen, L.I. Rossi, R.H. de Rossi, Appl. Catal. A Gen. 312 (2006) 120–124.
[10] A. Shahid, S. Lopez-Orozco, V.R. Marthala, M. Hartmann, W. Schwieger, Microporous Mesoporous Mat. 237 (2017) 151–159.
[11] A. Corma, Chem. Rev. 97 (1997) 2373–2419.
[12] Y. Zhang, C. Liu, B. Xu, F. Qi, W. Chu, Appl. Catal. B Environ. 199 (2016) 447–457.
[13] M.L. Rache, A.R. García, H.R. Zea, A.M.T. Silva, L.M. Madeira, J.H. Ramírez, Appl. Catal. B Environ. 146 (2014) 192–200.
[14] C. Saux, L. Pierella, Appl. Catal. A Gen. 400 (2011) 117–121.
[15] C. Saux, C.L. Marchena, L.R. Pizzio, L.B. Pierella, J. Porous Mater. 23 (2016) 947–956.
[16] A. Córdoba, N. Alasino, M. Asteasuain, I. Magario, M.L. Ferreira, Chem. Eng. Sci. 129 (2015) 249–259.
[17] N.A.S. Ramli, N.A.S. Amin, Chem. Eng. J. 283 (2016) 150–159.
[18] C. Hahn, S. Füger, M. Endisch, A. Pacher, S. Kureti, Global Kinetic Modelling of the NH3 Oxidation on Fe/BEA Zeolite, (2015).
[19] M.A.J.S. BOEKEL, J. Food Sci. 61 (1996) 477–486.
[20] C. Cabrera, A. Cornaglia, A. Córdoba, I. Magario, M.L. Ferreira, Chem. Eng. Sci. 161 (2017).
[21] 1972 P. Chu, 979, No Title, US Patent No. 3.709., 1972.
[22] J.P.P. S. Valencia, M.A. Camblor Fernández, A. Corma, Síntesis de Zeolita Beta, U.S. Patent 2 124 142, 1999.
[23] J. Ramírez, L.A. Godínez, M. Méndez, Y. Meas, F.J. Rodríguez, J. Appl. Electrochem. 40 (2010) 1729–1736.
[24] L. Singh, P. Rekha, S. Chand, Sep. Purif. Technol. 170 (2016) 321–336.
[25] J.F. Perez-Benito, Monatshefte Für Chemie/Chem. Mon. 132 (2001) 1477–1492.
[26] F.L.Y. Lam, A.C.K. Yip, X. Hu, Ind. Eng. Chem. Res. 46 (2007) 3328–3333.
[27] A.D. Bokare, W. Choi, J. Hazard. Mater. 275 (2014) 121–135.
[28] E.G. Garrido-Ramírez, B.K. Theng, M.L. Mora, Appl. Clay Sci. 47 (2010) 182–192.
[29] Jun Wang, Jung-Nam Park, Han-Cheol Jeong, Kwang-Sik Choi, Xian-Yong Wei, Suk-In Hong, Chul Wee Lee, (2004).
[30] W.B. Widayatno, G. Guan, J. Rizkiana, J. Yang, X. Hao, A. Tsutsumi, A. Abudula, Appl. Catal. B Environ. 186 (2016) 166–172.
[31] A. Sultana, T. Nanba, M. Haneda, M. Sasaki, H. Hamada, Appl. Catal. B Environ. 101 (2010) 61–67.
[32] J.H. Kwak, D. Tran, S.D. Burton, J. Szanyi, J.H. Lee, C.H.F. Peden, J. Catal. 287 (2012) 203–209.
[33] S. Kieger, G. Delahay, B. Coq, B. Neveu, J. Catal. 183 (1999) 267–280.
[34] S.A. Bates, A.A. Verma, C. Paolucci, A.A. Parekh, T. Anggara, A. Yezerets, W.F. Schneider, J.T. Miller, W.N. Delgass, F.H. Ribeiro, J. Catal. 312 (2014) 87–97.
[35] C. Paolucci, J.R. Di Iori, F.H. Ribeiro, R. Gounder, W.F. Schneider, Adv. Catal. 59 (2016) 1107–2016.
[36] C. Paolucci, A.A. Parekh, I. Khurana, J.R. Di Iorio, H. Li, J.D. Albarracin Caballero, A.J. Shih, T. Anggara, W.N. Delgass, J.T. Miller, F.H. Ribeiro, R. Gounder, W.F. Schneider, J. Am. Chem. Soc. Chem. Soc. 138 (2016) 6028–6048.
[37] F. Göltl, C. Michel, P.C. Andrikopoulos, A.M. Love, J. Hafner, I. Hermans, P. Sautet, ACS Catal. 6 (12) (2016) 8404–8409.
[38] F. Göltl, A.M. Love, I. Hermans, J. Phys. Chem. C 121 (2017) 6160–6169.
[39] E. Yuan, K. Zhang, G. Lu, Z. Mo, Z. Tang, J. Ind. Eng. Chem. 42 (2016) 142–148.
[40] V. Sundaramurthy, N. Lingappan, J. Mol. Catal. A Chem. 160 (2000) 367–375.
[41] D. Dumitriu, R. Bârjega, L. Frunza, D. Macovei, T. Hu, Y. Xie, V.I. Pârvulescu, S. Kaliaguine, J. Catal. 219 (2003) 337–351.
[42] S. Huang, Y. Wang, Z. Wang, B. Yan, S. Wang, J. Gong, X. Ma, Appl. Catal. A Gen. 417 (2012) 236–242.
[43] J.C. van der Waal, H. van Bekkum, J. Mol. Catal. A Chem. 124 (1997) 137–146.
[44] A. Corma, P. Esteve, A. Martínez, J. Catal. 161 (1996) 11–19.
[45] H. Liu, Z. Wang, H. Hu, Y. Liang, M. Wang, J. Solid State Chem. 182 (2009) 1726–1732.
[46] S. Lin, M.D. Gurol, Environ. Sci. Technol. 32 (1998) 1417–1423.
[47] R. Andreozzi, V. Caprio, R. Marotta, J. Chem. Technol. Biotechnol. 76 (2001) 196–202.
[48] R.D. Bach, M.-D. Su, H.B. Schlegel, J. Am. Chem. Soc. 116 (1994) 5379–5391.
[49] S.H. Lin, M.Lin chi, H.G. Leu, Operating Characteristics and Kinetic Studies of Surfactant Wastewater Treatment by Fenton Oxidation, (1999).
[50] S.-P. Sun, C.-J. Li, J.-H. Sun, S.-H. Shi, M.-H. Fan, Q. Zhou, J. Hazard. Mater. 161 (2009) 1052–1057.
[51] J.-H. Sun, S.-P. Sun, M.-H. Fan, H.-Q. Guo, L.-P. Qiao, R.-X. Sun, J. Hazard. Mater. 148 (2007) 172–177.
[52] R. Atkinson, R.A. Perry, J.N. Pitts, J. Chem. Phys. 66 (1977) 1578–1581.
[53] K.H. Schmidt, J. Phys. Chem. 81 (1977) 1257–1263.